Zero-Field Splitting of the Electronic Ground and Lowest Excited Triplet States of 2,2-Dinaphthylcarbene in *n*-Hexane at 1.7 K

B. Kozankiewicz*,† and M. Aloshyna

Institute of Physics, Polish Academy of Sciences, Al. Lotników 32/46, 02 668 Warsaw, Poland

A. D. Gudmundsdottir and M. S. Platz*

Department of Chemistry, The Ohio State University, Columbus, Ohio 43210

M. Orrit* and Ph. Tamarat

Centre de Physique Molèculaire Optique et Hertzienne, CNRS et Universite Bordeaux I, 351 Cours de la Liberation, 33405 Talence Cedex, France

Received: December 2, 1998; In Final Form: February 12, 1999

The triplet−triplet fluorescence spectra of a new carbene, 2,2-dinaphthylcarbene in *n*-hexane and *n*-heptane, were studied at cryogenic temperatures. Synthesis of the carbene precursor, 2,2-dinaphthyldiazomethane, is described. Spectral holes were burned within the inhomogeneous 0,0 fluorescence excitation line assigned to the pseudo-E/trans conformer. The complicated pattern of burned holes was interpreted with a model taking into account the zero-field splitting (ZFS) of the ground T_0 and excited T_1 triplet states and the selectivity of the intersystem crossing channel. The unusual observation of antiholes was attributed to the extremely long spin−lattice relaxation time in the T_0 state. The analysis provided direct information about the ZFS parameters of the T_0 and T_1 states: $E_0 = 0.022 \pm 0.001$ cm^{-1}, $D_0 = 0.477 \pm 0.001$ cm^{-1}, $E_1 = 0.006 \pm 0.0002$ cm^{-1}, and $D_1 = 0.043 \pm 0.0005$ cm^{-1}.

I. Introduction

Carbenes play a very important role in organic chemistry as short-lived intermediates produced in many chemical reactions.[1] They can be created from the appropriate diazo, diazirine, and/or ketene precursors by photolysis with visible or UV light. Experimental studies of reactive intermediates present a challenge because their concentration in either the gas or liquid phase at room temperature is extremely small. This problem can be avoided, however, by using matrix isolation techniques. In a cryogenic matrix, friction greatly restricts molecular motion and effectively eliminates intramolecular and intermolecular reactions. Thus, under these conditions it is possible to produce a relatively large and stable concentration of carbenes and study them for many days, in practice as long as the matrix is kept frozen.

Carbenes have two nonbonding electrons and, depending on their molecular structure, may have either a triplet or singlet electronic ground state. Information about the geometry and electronic structure of triplet carbenes can be obtained by EPR, electronic absorption, and emission spectroscopy of carbenes immobilized in matrix hosts.[2−4] In a low-temperature Shpolskii matrix the $T_1 \rightarrow T_0$ fluorescence and $T_0 \rightarrow T_1$ fluorescence excitation spectra[4] are often composed of sharp, zero-phonon quasi-lines accompanied by broad phonon wings. These quasi-lines are inhomogeneously broadened because of the slightly different environments of the ensemble of carbenes produced in a polycrystalline matrix providing a convenient situation for hole-burning studies using highly selective irradiation with a narrow-band ring dye laser.

* Corresponding author.
† E-mail: kozank@ifpan.edu.pl. Fax: (+48-22) 8430926.

The first successful hole-burning experiment on the 0,0 line of a $T_0 \rightarrow T_1$ fluorescence excitation spectrum was recently performed on 2-naphthylphenylcarbene (2NPC) dispersed in *n*-hexane and *n*-heptane at 1.7 K.[5,6] A complicated pattern of holes was explained when taking into account the zero-field splitting (ZFS) of the T_0 and T_1 states and some assumptions about the energy dissipation channels. The ZFS of triplet states originates from the spin−spin interaction between two unpaired electrons and contains important information about the spatial distribution of these electrons. The analysis of hole-burning spectra provided the ZFS parameters of both the T_0 and T_1 states. This information is not generally available for the excited, short-lived T_1 state of a carbene.

In the present work we have undertaken spectroscopic studies of a new aromatic carbene, 2,2-dinaphthylcarbene. This compound can exist in two different conformations (rotameric forms), which we will call pseudo-E/trans and pseudo-Z/cis conformers.

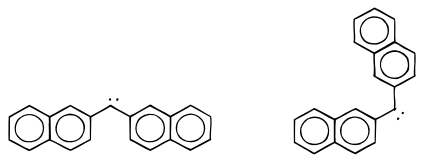

pseudo-E/trans pseudo-Z/cis

II. Experimental Section

A. Synthesis of 2,2-Dinaphthyldiazomethane. Synthesis of 2,2-dinaphthyldiazomethane (in Columbus) and characterization of intermediate steps are described below.

10.1021/jp984581e CCC: $18.00
Published on Web 04/08/1999

Preparation of Di-2-naphthalenylmethanone. Di-2-naphthalenylmethanone was prepared by the method of Olah et al.[7] Piperidine (10 mL, 0.10 mol) was added dropwise to a solution of ethyl chloroformate (5 mL, 0.05 mol) in diethyl ether (25 mL) at −78 °C under argon. The resulting solution was stirred at ambient temperature for an hour and refluxed for another hour. The reaction was quenched by addition of water. The organic layer was washed with water, dried over sodium sulfate, the solvent removed under vacuum, and the residue distilled under vacuum to yield *N*-carboethoxypiperdine (5.8 g, 0.037 mol, 71% yield). IR (NaCl plates, neat) ν_{max}: 2981, 2936, 2855, 1698, 1432 cm^{-1}. ^1H NMR ($CDCl_3$, 200 MHz): δ 4.05 (q, 7 Hz, 2H, 3.40 (m, 4H), 1.5 (m, 6H), 1.20 (t, 7 Hz, 3H) ppm. MS (*m*/*e* relative intensity): 157 (M^+, 10), 156 (100), 128 (40), 84 (84). High-resolution mass calculated for $C_8H_{15}NO_2$: 157.1103. Found 157.1075.

A solution of *N*-carboethoxypiperidine (1.0 g, 0.073 mmol) in diethyl ether (15 mL) was added to a dispersion of 2-lithium naphthalene in diethyl ether at 0 °C under argon. This mixture was stirred for half an hour at room temperature and then refluxed for an hour. The reaction was quenched by addition of 10% aqueous HCl (20 mL), and ethyl acetate (50 mL) was added. The organic layer was washed with saturated sodium bicarbonate solution and brine solution and dried over $MgSO_4$ and the solvent removed under vacuum to give an off-white solid (2 g). The resulting solid was recrystallized from an ethyl acetate−hexane mixture to yield colorless plates of di-2-naphthalenylmethanone (1.1 g, 4 mmol, 54% yield) and a mother liquor that contained a mixture of di-2-naphthalenylmethanone and some unreacted 2-bromonaphthalene (0.88 g).

The 2-lithium naphthalene was prepared by adding butyllithium to an ether solution of 2-bromonaphthalene at ambient temperature. The solution was stirred for 15 min and then refluxed for half an hour; mp 157−8 °C (lit.[8] 125 °C). IR ($CHCl_3$)ν_{max}: 1654, 1627, 1288 cm^{-1}. ^1H NMR ($CDCl_3$, 200 MHz): δ 8.33 (s, 2H), 8.0 (s, 4H), 7.9 (m, 4H), 7.60 (d of quint, 2 and 7 Hz, 4H) ppm. ^{13}C NMR ($CDCl_3$, 75 MHz): δ 196.7 (C═O), 135.2 135,1 132.3, 131.8 129.4, 128.3, 128.2, 127.8, 126.8, 125.9 ppm. MS (*m*/*e*, relative intensity): 282 (M^+, 81), 254 (30), 155 (100), 127 (89). Mass calculated for $C_{21}H_{14}O$: 282.1045. Found: 282.1048.

Preparation of (Di-2-naphthalenylmethane)hydrazide-4-methylbenzenesulfonic Acid. Di-2-naphthalenylmethanone (1.11 g, 3.9 mol) and tosylhydrazone (0.74 g, 3.9 mol) were dissolved in toluene and refluxed under argon overnight. The solvent was removed under vacuum, and the resulting solid was recrystallized from ethanol to yield colorless needles of (2,2-naphthalenylmethane)hydrazide-4-methylbenzenesulfonic acid (1.41 g, 3.1 mole, 80% yield); mp 188−190 °C. IR (KBr) ν_{max}: 3289, 1387, 1166 cm^{-1}. ^1H NMR ($CDCl_3$, 200 MHz): δ 8.1−7.8 (m, 8H), 7.7−7.6 (m, 5H), 7.5−7.3 (m, 5H), 7.22 (dd, 8.5 and 1.6 Hz, 1H), 2.45 (s, 3H, $-CH_3$) ppm. ^{13}C NMR ($CDCl_3$, 75 MHz): δ 154.4, 144.2, 135.6, 134.1, 134.0, 133.7, 133.3, 132.7, 130.0, 129.7, 129.0, 128.4, 128.4, 128.1, 128.1, 128.0, 127.7, 127.6, 127.3, 127.1, 126.4, 125.1, 123.8 ppm. MS (*m*/*e*, relative intensity): 450 (M^+, 81), 254 (30), 155 (100), 127 (89). Mass calculated for $C_{28}H_{22}N_2O_2S$: 450.14036. Found: 450.13824.

Preparation of Di-2-naphthyldiazomethane. Di-2-naphthyldiazomethane was prepared by following a method by Jonczyk et al.[9] (Di-2-naphthalenylmethane)hydrazide-4-methylbenzenesulfonic acid was dissolved in dioxane (40 mL) and sodium hydroxide (2 mL, 50% in water) added to the solution. The reaction mixture was stirred and heated at 85 °C for an hour. The resulting solution was cooled to room temperature. The water layer was extracted with pentane, and the combined organic layers washed with brine, dried over $MgSO_4$, and concentrated under vacuum. The resulting red solid was recrystallized two times from pentane; mp (uncorrected) 123−124 °C. IR (KBr) ν_{max}: 2021, 1625, 1595 cm^{-1}. ^1H NMR ($CDCl_3$, 200 MHz): δ 8.0−7.5 (m, 14H) ppm. ^{13}C NMR ($CDCl_3$, 50 MHz): δ 133.9, 131.8, 128.9, 128.4, 127.8, 127.3, 127.0, 126.7, 125.7, 123.7, 123.4 ppm.

B. Experimental Setup. The 2,2-dinaphthylcarbene (22-DNC) sample was obtained "in situ" by the photolysis of the 2,2-dinaphthyldiazomethane precursor dispersed in a Shpolskii matrix of *n*-hexane or *n*-heptane at 5 K. The 366 nm line, isolated by appropriate filters from the spectrum of a mercury lamp, was used during this procedure. Before being inserted into the liquid helium cryostat, all samples were degassed by the "freeze−pump−thaw" technique. Samples of 22-DNC were annealed overnight, when the cryostat was warmed slowly to approximately 100 K, and subsequently cooled back the next day to the temperature of boiling liquid helium.

The fluorescence and fluorescence excitation spectra (in Warsaw) were measured using two different experimental techniques. In the photon-counting configuration the samples were excited either with the 366 nm line isolated from the spectrum of a HBO200 mercury lamp or with the light emitted by a Coherent 700 dye laser pumped by a mode-locked Coherent Antares 76 Nd:YAG laser. In the latter case the laser was scanned within the lasing frequency range of rhodamine 6G dye, between 570 and 600 nm. Emission spectra were observed at the right angle using a 0.25 m Jarrel-Ash monochromator and an EMI 9659 photomultiplier, cooled to −20 °C and operating in the photon-counting mode. A LightScan PC card was used as the pulse-counting electronics and as the master clock of the experiment. In the photon-sampling configuration the excitation source was a Lambda Physik FL 1001 dye laser pumped by an LPX 100 excimer laser. Coumarin 153 was the lasing dye for the spectral range 530−600 nm and rhodamine B for the range 595−640 nm. Fluorescence light was detected with the aid of an EMI 9659 photomultiplier and a Stanford Research SR250 boxcar averager connected to a previously mentioned PC card.

Fluorescence decays were measured using the "time-correlated" single-photon-counting technique. The samples were excited in this case by the previously mentioned Coherent laser system, which provided light pulses with about a 20 ps pulse width and a 3.8 MHz repetition rate. Start and stop signals were detected by an avalanche photodiode and a Hamamatsu R28090-07 microchannel plate photomultiplier, respectively. A Tennelec TC 454 quad constant fraction discriminator, a TC 864 time-to-amplitude converter, and a Nucleus PCA-II multichannel analyzer card were used. The estimated time resolution of this setup was about 50 ps.

The optical hole-burning setup (of the Bordeaux Laboratory) used a single-mode dye laser Coherent CR 699-21 with 1−3 MHz frequency resolution and 30 GHz scan width. The lasing dye was rhodamine 6G. The laser light was stabilized with the aid of an electrooptic modulator Conoptics Lass-II. Holes were burned with light intensity between 0.1 and 0.01 mW/cm^2 over a burning time between 100 and 500 s. The monitoring intensity was about 10 times weaker than that when burning holes. The fluorescence light emitted from the sample was collected by an achromatic lens and focused on the slit of a small monochromator (with spectral resolution of a few nanometers). A monochromator was used to select the main vibronic line separated by 1353 cm^{-1} from the 0,0 origin of the fluorescence.

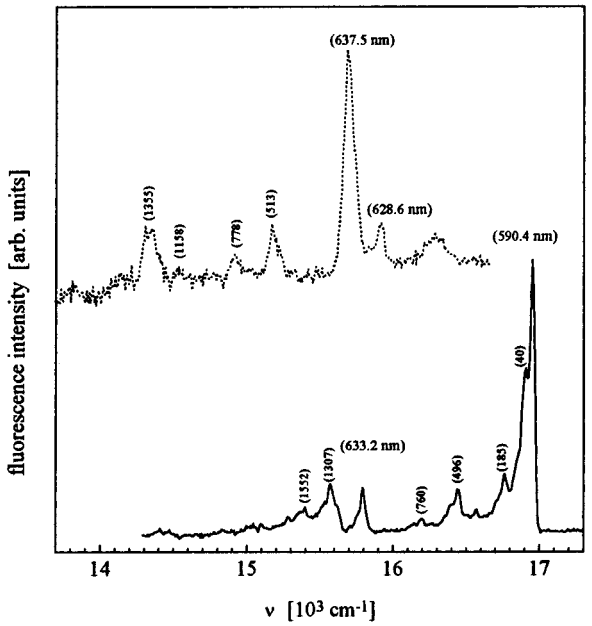

Figure 1. Fluorescence spectra of 22-DNC in *n*-hexane (solid line) and in *n*-heptane (dotted line) at 5 K. The wavelength of excitation light in both cases was 366 nm. The spectra presented are typical for the annealed samples.

The excitation light, which was scattered off the sample, was further removed with a RG630 Schott glass filter. An RCA 31034-A02 photomultiplier, cooled to −20 °C and operating in the photon-counting mode was used to detect the light.

III. Results

A. Fluorescence and Fluorescence Excitation Spectra of 22-DNC. The fluorescence spectra of 22-DNC in Shpolskii matrices of *n*-hexane and *n*-heptane at 5 K, when excited by the 366 nm line to a higher excited triplet state, are shown in Figure 1. The spectra can be attributed to the two main conformers of 22-DNC. By analogy to 2-NPC,[10] we can presume that the pseudo-E/trans conformer absorbs at higher energy and contributes to the spectrum with the 0,0 origin at about 590 nm whereas the pseudo-Z/cis contributes to the spectrum with the 0,0 band around 635 nm. It has been experimentally observed that the former conformer dominates in the *n*-hexane matrix and that the latter is the only one present in frozen *n*-heptane.

The spectra of both conformers are composed of narrow vibronic lines that can be resolved by using appropriate laser excitation. With the selective laser excitation of the main vibronic component of the T_1 state of 22-DNC in *n*-hexane, 1343 cm^{-1} (λ_{exc} = 546.9 nm) for the high energy and 1312 cm^{-1} (λ_{exc} = 585.2 nm) for the low-energy conformer, the fluorescence spectra can be separated, as shown in Figure 2. The respective 0,0 fluorescence origins are located at 590.4 and 633.7 nm. The spectral resolution of the fluorescence spectra presented is limited by the monochromator (half-bandwidth above 30 cm^{-1}). The fluorescence excitation spectra, observed at the main vibronic component of fluorescence at 1353 cm^{-1} (λ_{obs} = 643 nm) and measured with a laser spectral resolution of 0.2 cm^{-1}, are much more narrow. They are composed of sharp quasi-lines, and the 0,0 origins of the fluorescence and fluorescence excitation spectra coincide. Both of these observations indicate that the spectrum of 22-DNC in Shpolskii matrix is composed of zero-phonon lines. Thus, the system seems to be a good candidate for hole-burning experiments.

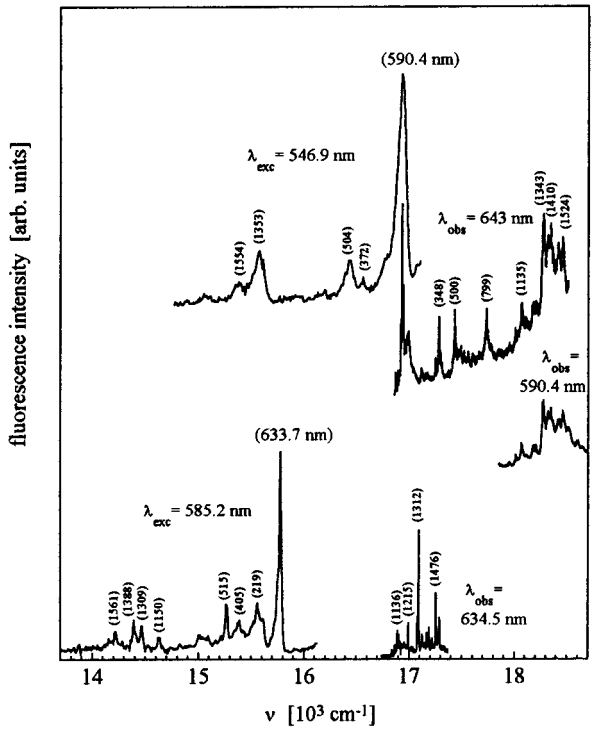

Figure 2. Fluorescence and fluorescence excitation spectra of 22-DNC in *n*-hexane at 5 K after the sample was annealed. The wavelengths of excitation (in the case of the fluorescence spectrum) and wavelengths of observation (in the case of the fluorescence excitation spectrum) are indicated above the spectra. The numbers in parentheses indicate the vibrational frequencies (given in cm^{-1}) of the 0,0 origins of both main conformers (given in nanometers).

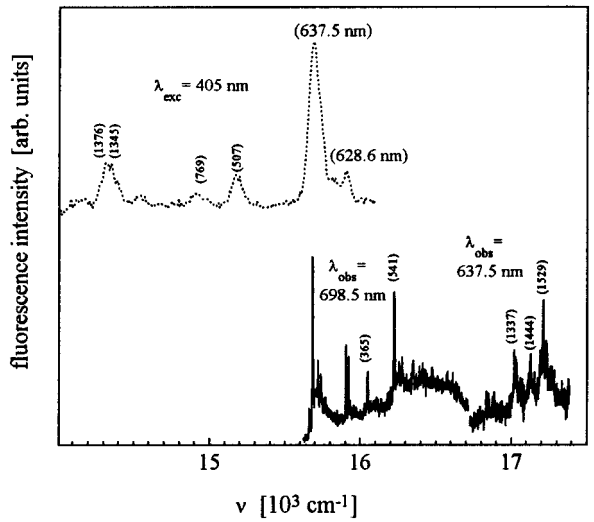

Figure 3. Fluorescence and fluorescence excitation spectra of 22-DNC in *n*-heptane at 5 K after the sample was annealed. The wavelength of excitation (in the case of the fluorescence spectrum) and the wavelengths of observation (in the case of the fluorescence excitation spectrum) are indicated above the spectra. The numbers in parentheses indicate the vibrational frequencies (given in cm^{-1}) of the 0,0 origins (given in nanometers).

The fluorescence and fluorescence excitation spectra of 22-DNC in *n*-heptane are shown in Figure 3. The origins of fluorescence and fluorescence excitation lines coincide at 637.5 and 628.6 nm. These lines can be identified with the low-energy conformer, presumably pseudo-Z/cis. In the *n*-heptane matrix we were not able to observe any line that can be assigned to the high-energy conformer. The pseudo-E/trans conformer should have its origin at around 590 nm.

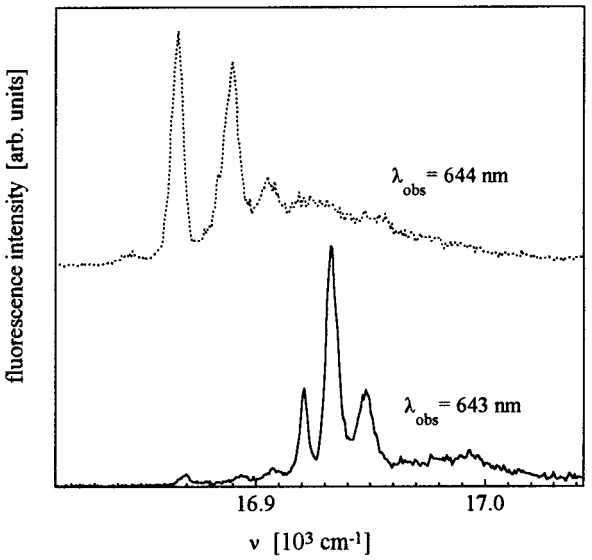

Figure 4. The 0,0 fluorescence excitation bands of 22-DNC in *n*-hexane at 4.2 K measured just after photolysis (dotted line) and the next day, after annealing at 100 K (solid line).

The spectra presented in Figures 2 and 3 were collected for the annealed samples. However, it is a characteristic feature of the high-resolution spectroscopy of carbenes that the spectrum depends on the thermal treatment of the sample and the spectrum changes after annealing. This phenomenon is illustrated in Figure 4. The 0,0 fluorescence excitation origin lines of the high-energy conformer of 22-DNC in *n*-hexane at 5 K, observed at 16 866 and 16 890 cm^{-1} before annealing, rearrange to higher energy after the overnight annealing, and the main line is located at 16 933 cm^{-1}. After the annealing procedure the fluorescence spectrum shifts to higher energy (by about 60 cm^{-1}) as well. The observed spectral changes reflect a rearrangement of the 22-DNC geometry from one resembling that of its precursor, 22-dinaphthyldiazomethane, to the geometry of the relaxed 22-DNC.

B. Fluorescence Decays. Fluorescence decays for both conformers of 22-DNC in *n*-hexane matrix at 5 K are shown in Figure 5. All of the decays were nonexponential as observed previously for many other carbenes.[4,10,11] This phenomenon has been interpreted as a result of different intersystem crossing rates from the three triplet sublevels of the T_1 state that were manifested by a triexponential fluorescence decay. Since the transition moments are spin-independent, the radiative rate constants for the three spin sublevels should be equal and the excitation pulse should equally populate the three spin sublevels of the T_1 state. Thus, the experimental decays are expected to be a sum of three exponential decays with the same preexponential factors. The above consideration does not take into account the Boltzman population of the spin sublevels of the T_0 state. By use of the energy spacing between these spin sublevels (T_{0x} and T_{0y} are 0.455 and 0.499 cm^{-1} above the lowest energy T_{0z} sublevel; this spacing will be found in the following part of this work), the relative Boltzman populations of the spin sublevels at 5 K are 1:0.876:0.865. Because of the lack of symmetry of 2,2-DNC, the electronic transition from each spin sublevel of the T_0 state to each of the T_1 state is possible.

Therefore, we considered two possible situations and fitted the decays with a three-exponential function with the same preexponential factors and with a function where preexponential factors were proportional to the Boltzman population. In each case there were four fitting parameters. The best fits are shown in Figure 5. The crucial conditions to be met to obtain a successful fitting (convolution with the excitation pulse) were high-quality decay curves (to fulfill this requirement, we collected the decay curves up to 10^4 counts in maximum) and a precise estimation of the baseline. Under these conditions, the iterative, nonlinear least-squares fitting program found that the best approximation of the decays was a three-exponential decay with the preexponential factors proportional to the Boltzman population and with the component decay times of 5.9, 28.1, and 28.1 ns for the pseudo-E/trans conformer and 7.0, 7.0, and 15.6 ns for the pseudo-Z/cis conformer. In the case of fitting by three-exponential decays with the same preexponential factors, the fitting quality was acceptable but not as good as in the above case (as judged by slightly higher value of the χ^2 and less equilibrated residual plot), but the decay components are very similar: 5.8, 27.8, and 27.8 ns for the pseudo-E/trans and 7.0, 7.0, and 15.6 ns for the pseudo-Z/cis

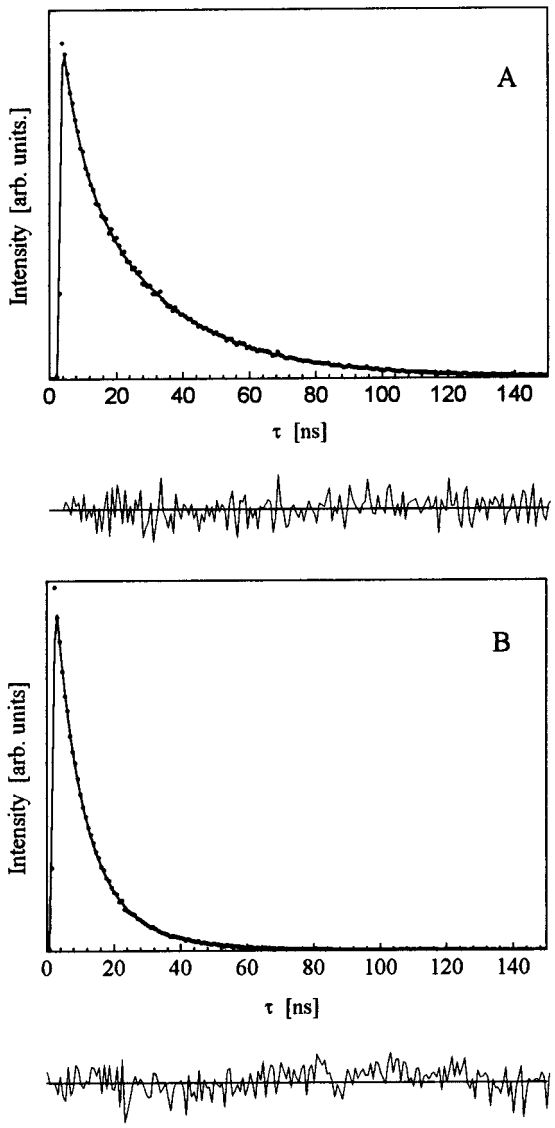

Figure 5. Fluorescence decays of 22-DNC in *n*-hexane at 5 K: (A) λ_{exc}= 590.4 nm, λ_{obs} = 643 nm corresponds to the pseudo-E/trans, in which the best fit is given by the dependence (where *t* is in nanoseconds) $0.0405 \exp(-t/5.9) + 0.036 \exp(-t/28.1) + 0.0355 \exp(-t/28.1)$; (B) λ_{exc} = 585 nm, λ_{obs} = 633.7 nm, corresponds to the pseudo-Z/cis conformer, in which the best fit is given by the dependence $0.049 \exp(-t/7.0) + 0.0436 \exp(-t/15.6) + 0.043 \exp(-t/7.0)$. Plots of residuals of a least-squares fit to a three-exponential decay dependence are added below the decays.

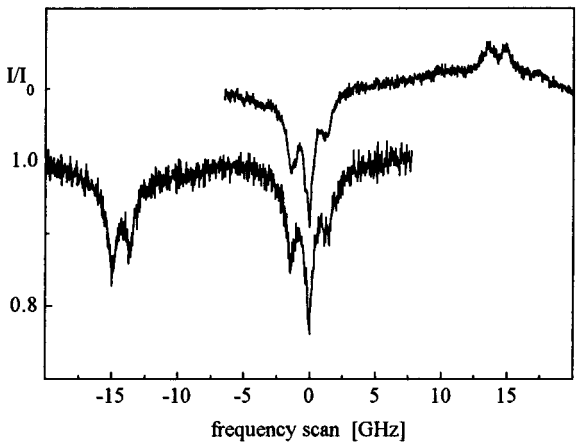

Figure 6. Typical holes burned within the inhomogeneous 0,0 fluorescence excitation line (around 16 900 cm^{-1}) of 22-DNC in *n*-hexane at 1.7 K. The spectral positions of holes are given with respect to the frequency of the burning light. The scanning range was limited to 30 GHz, and therefore, the low- and high-energy sides of the hole spectrum required separate detection.

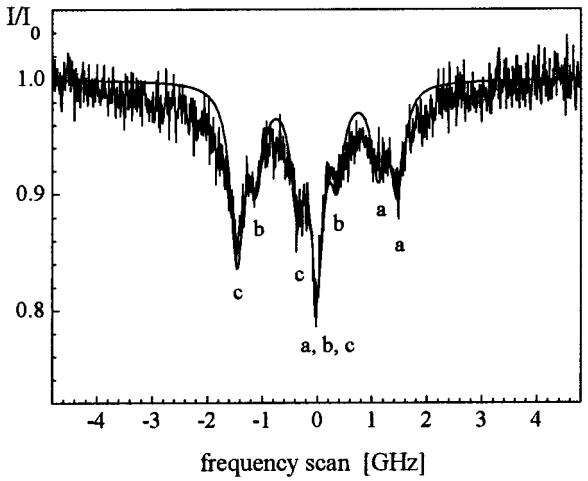

Figure 7. Detdetailed structure of holes in the central part of hole-burning spectrum. Holes are assigned by the same letters as in the spectrum of holes in the model presented in Figure 9. The fit by seven Lorentzians is given by the solid line. The Lorentzian parameters are collected in Table 1.

conformer. The precise value of each decay component changed slightly with varying pulse and decay baselines, but one decay component was always different from the other two, which were approximately the same. The result indicates that in the case of the pseudo-E/trans conformer the spin−orbit interaction efficiently couples a singlet manifold with one spin sublevel of the T_1 state and that this sublevel is depopulated more rapidly than the other two.

The above results suggest that the fluorescence decay curves in the case of 22-DNC should be well approximated by a biexponential dependence. Therefore, we also fitted the decays with a biexponential function and found that fits were even better, the χ^2 values were smaller, than in the case when we approximated decays by the sum of three exponentials. The best fits to a biexponential dependence were given by $0.042 \exp(-t/6.1) + 0.069 \exp(-t/27.6)$ for the pseudo-E/trans and $0.103 \exp(-t/7.7) + 0.030 \exp(-t/17.2)$ for the pseudo-Z/cis conformer.

C. Hole-Burning Experiments. Hole-burning experiments were performed on the 0,0 fluorescence excitation line, which has its maximum at 16 933 cm^{-1} with a full width at half of maximum (fwhm) of about 6 cm^{-1}. It was attributed to the high energy pseudo-E/trans conformer of 22-DNC. This conformer dominated the spectrum in *n*-hexane and was absent in *n*-heptane. In the present experimental configuration we were not able to extend the hole-burning studies to the low-energy conformer of 22-DNC because our single-mode dye laser system was limited to the lasing range of rhodamine 6G (570−620 nm range). Hole-burning studies with the low-energy conformer will be the subject of forthcoming investigations.

A typical pattern of holes, burned within the inhomogeneous 16 933 cm^{-1} line of the 0,0 fluorescence excitation, is shown in Figure 6. The central hole, burned at the frequency of the applied laser light, had a fwhm of about 0.3 GHz and a depth of 25% (after prolonged burning we were able to create hole of a depth reaching 50%). Several substructures appeared around this line in a frequency range of −2 to +2 GHz, and this part of the hole-burning spectrum is presented in Figure 7. Two satellite holes of similar width were located on both sides of the central hole, 0.36 ± 0.01 GHz away. Two other pairs of satellite holes, separated by 0.35 ± 0.01 GHz within the pair, were located 1.11 ± 0.01 GHz from the center of the spectrum. When we scanned a broader frequency range around the central hole (Figure 6), we found a pair of deep holes at −13.65 ± 0.05 and −14.95 ± 0.05 GHz and a pair of antiholes at 13.6 ± 0.1 and 14.9 ± 0.1 GHz. The area of antiholes on the high-energy side was much smaller than that of the deep holes on the low-energy side.

IV. Discussion

The observed complicated pattern of holes can be explained when taking into account the zero-field splitting (ZFS) of the T_0 and T_1 states.

The ZFS parameter D is proportional to $\langle 1/r^3 \rangle$, where r is the average separation between the two unpaired electrons and depends therefore on the distribution of these electrons. In the electronic ground state, T_0, of carbenes, both unpaired electrons are localized on the central carbene atom, one electron occupying a σ orbital and the other a π orbital.[2,3] This implies that the ZFS parameter D_0 has a large value. In the excited T_1 state, one of the unpaired electrons is substantially delocalized onto the naphthalene ring (occupying a π^* orbital), whereas the second one remains on the carbenic center.[4,12] Consequently, the average separation of the two unpaired electrons is much larger in the T_1 than in the T_0 state and the D_1 parameter is small, much smaller than the D_0 value. It is therefore reasonable to predict that the holes and antiholes located far from the central hole (13−15 GHz away) should reflect the ZFS of the ground T_0 state, whereas the holes located in the neighborhood of the central hole (within the ±2 GHz range) should reflect the ZFS of the excited T_1 state.

Let us first consider the simplified situation where we can neglect a splitting of the T_1 state. The energy level scheme for this situation is shown in Figure 8. We used the axis convention of Brandon et al.,[13] where the *z* axis passed through the central carbene atom being parallel to the line joining the centers of the two adjacent carbon atoms and the *x* axis was perpendicular to the plane defined by these three carbons. The order and relative separations of the ZFS sublevels of the ground state, T_{0z}, T_{0x}, and T_{0y}, were assumed to be the same as that established from electron spin echo experiments for diphenylcarbene.[14] Among the molecules that contribute to the inhomogeneous 0,0 fluorescence excitation line, the hole-burning laser light can interact only with three groups of molecules, those that have the same $T_{0z} \rightarrow T_1$, $T_{0x} \rightarrow T_1$, and $T_{0y} \rightarrow T_1$ transition energy

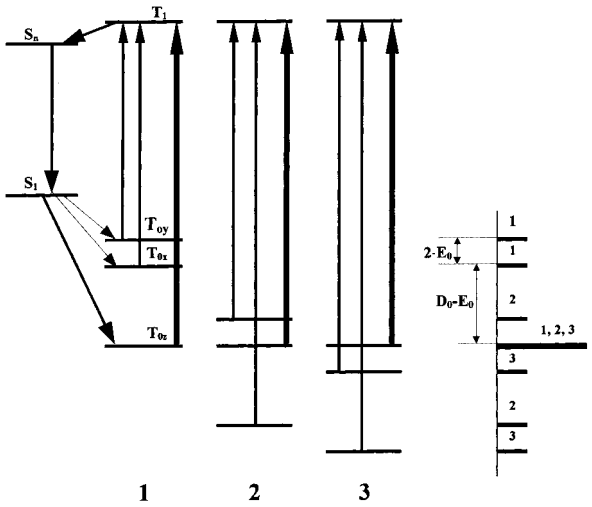

Figure 8. Energy level schemes and the main electronic transitions considered in the text. The thick lines indicate the burning transitions resonant with laser light. The schemes in this figure neglect the ZFS of the excited T_1 state. Spectral positions of the possible absorption transitions (and holes) of the three groups of molecules, which can be in resonance with a laser frequency, are shown on the right side of the figure.

(in Figure 8 the transitions resonant with the laser light are indicated by thick lines). If the burning efficiency is the same for these three groups of molecules, the central hole should be surrounded by three holes on the high- and three on the low-energy side. The experimental hole spectrum differs from these predictions. The observed pair of holes located on the low-energy side of the central hole can be created by molecules from group 1 only, whereas the antiholes, located on the high-energy side of the central hole, are derived from molecules from groups 2 and 3.

22-DNC seems to be photochemically stable in low-temperatures matrices; we were able to study this compound for several days (burning new holes after the overnight annealing) with no detectable drop of the total emission intensity. The hole-burning process should therefore be nonphotochemical and proceed via nonradiative relaxation channels. The relaxation energy, when dissipated to the matrix surrounding the molecule, can change the molecule−matrix local configuration, leading to a new energy minimum. Consequently, the zero-phonon line of the carbene can be spectrally shifted, leaving a spectral hole at the previous position. The following discussion provides arguments that this is the mechanism of burning holes in the 0,0 fluorescence excitation line of 22-DNC. There are two possible channels of nonradiative relaxation, the $T_1 \rightarrow T_o$ internal conversion and the $T_1 \rightarrow S_n \rightarrow S_1 \rightarrow T_0$ intersystem crossing. The former process does not differentiate among the three groups of molecules under consideration. The latter process is known to be highly selective for different ZFS triplet components, and if dominant, it may explain the observed pattern of burned holes. Let us first consider the consequence of high selectivity of the final step, $S_1 \rightarrow T_0$, in the intersystem crossing pathway. In the T_0 and S_1 states of carbenes (a good prototype is methylene, CH_2) both unpaired electrons are localized on the central carbene atom, occupying $(p_x)^1(sp_y)^1$ and $(p_x)^2$ orbitals, respectively. One center spin−orbit coupling on carbon (the spin−orbit operator l transforms like a 90° rotation) can mix the T_0 and S_1 states only through the matrix elements whose orbital part has the form $\langle p_x|l_z|p_y\rangle$.[15] This implies that the $S_1 \rightarrow T_{0z}$ intersystem crossing channel dominates $S_1 \rightarrow T_{0x}$ and $S_1 \rightarrow T_{0y}$. The selective population of the T_{0z} sublevel was already experimentally demonstrated for diphenylcarbene[14] and 2-naphthylphenylcarbene.[5] If the molecules excited to the T_1 state have to relax to their T_{0z} sublevel, then the only group of molecules that can efficiently absorb many photons and be burned are those that have the $T_{0z} \rightarrow T_1$ transition in resonance with the laser (hole burning) light. Other groups of molecules (2 and 3) that also satisfy the energy resonance requirement are protected from burning as long as they are trapped in the T_{0z} state. Spin−lattice relaxation, which restores the Boltzman population of the spin sublevels, is usually very long at 1.7 K, and therefore, the number of photons that can be absorbed by molecules belonging to groups 2 and 3 is relatively small. We can even predict that instead of holes, we should observe temporal (on the time scale of spin−lattice relaxation time) antiholes, corresponding to the $T_{0z} \rightarrow T_1$ transition energies of molecules from groups 2 and 3. The observation of persistent antiholes that do not disappear for a long time (after 15 min we were not able to monitor any drop of intensity of antiholes presented in Figure 6) may indicate the existence of carbenes that are characterized by extremely long spin−lattice relaxation times. Probably this long relaxation time can be related to a large energy separation between the spin sublevels of the T_0 state, but this problem is not clear and needs further investigation. As a reminder, in the case of 2-naphthylphenylcarbene,[5] where the ZFS of the T_0 state is similar, we were not able to detect any antihole.

The spectral positions of deep holes (and antiholes) provide direct information about the ZFS of the T_0 state. The energy separations between the spin sublevels are

$$\Delta E(T_{0z},T_{0x}) = D_0 - E_0 = 13.65 \pm 0.05 \text{ GHz}$$

and

$$\Delta E(T_{0x},T_{0y}) = 2E_0 = 1.3 \pm 0.05 \text{ GHz}$$

These lead to

$$E_0 = 0.65 \pm 0.03 \text{ GHz} = 0.022 \pm 0.001 \text{ cm}^{-1}$$

$$D_0 = 14.3 \pm 0.03 \text{ GHz} = 0.477 \pm 0.001 \text{ cm}^{-1}$$

Discussion of the origin of satellite holes located in the neighborhood of the central hole is possible if we consider the ZFS of the excited T_1 state, which was neglected in the previous discussion. Distribution of the electronic density is different in the T_0 and T_1 state, and therefore, the principal spin axes x, y, and z in the T_0 state can rotate to new x', y', and z' axes in the T_1 state. Consequently, electronic transitions from each spin sublevel of the T_0 to each spin sublevel T_1 are possible.

In the following discussion we will limit our considerations to molecules that can be burned (and thus the origin of the spin sublevel in absorption is the T_{0z} state). Three possible transitions, $T_{0z} \rightarrow T_{1z'}$, $T_{0z} \rightarrow T_{1x'}$, and $T_{0z} \rightarrow T_{1y'}$, define three groups of molecules (1a, 1b, and 1c) that can efficiently interact with the laser hole-burning light. The corresponding energy level schemes and electronic transitions are shown in Figure 9. The model predicts that the group of molecules 1a should contribute to the central hole and to two holes on the high-energy side, group 1b to the central hole and to one hole on the high- and one on the low-energy side, and group 1c to the central hole and to two holes on the low-energy side of the central hole. The predicted pattern of holes is shown on the right side of Figure 9, and it can be compared with the spectrum of holes observed in the neighborhood of the central hole, shown in Figure 7. It

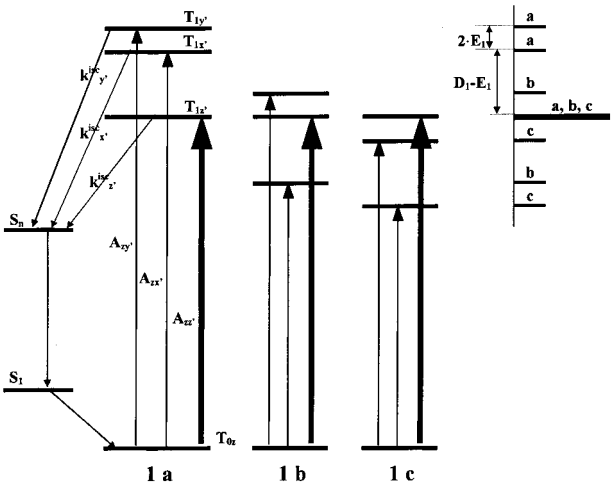

Figure 9. Energy level schemes and the electronic transitions that contribute to the spectrum of satellite holes surrounding the central hole. The thick lines indicate the burning transitions resonant with laser light. Spectral positions of absorption transitions (and holes) of the three groups of molecules, which can be in resonance with a laser frequency, are shown on the right side of the figure.

TABLE 1: Parameters of Seven Lorentzian Functions Adopted to Fit the Central Part of the Hole-Burning Spectrum Presented in Figure 9[a]

	ν_0 [GHz]	fwhm [GHz]	S
a	1.47	0.29	0.041
a	1.11	0.29	0.032
b	0.36	0.28	0.031
a, b, c	0.00	0.27	0.07
c	−0.36	0.28	0.043
b	−1.11	0.29	0.033
c	−1.47	0.29	0.068

[a] The sum of Lorentzians was given by the solid line in Figure 9. Each of the Lorentzian functions has been characterized by the formula $(2/\pi)Sw/(4(\nu - \nu_0)^2 + w^2)$, where fwhm is a full width at half of maximum, S is the area, and ν_0 is the frequency of the Lorentzian maximum.

is straightforward to identify the predicted holes and assign them according to the model. To go deeper into the origin of the burned holes, we fitted the experimental spectrum with seven Lorentzian curves as shown in Figure 7. The Lorentzian parameters (frequency at the maximum, ν_0; full width at half of maximum, fwhm; area, S) are collected in Table 1.

The frequencies at the maxima of the holes are directly related to the ZFS parameters D_1 and E_1 of the excited T_1 state:

$$\Delta E(T_{1z'},T_{1x'}) = D_1 - E_1 = 1.11 \pm 0.01 \text{ GHz}$$

$$\Delta E(T_{1x'},T_{1y'}) = 2E_1 = 0.36 \pm 0.01 \text{ GHz}$$

This gives

$$E_1 = 0.18 \pm 0.005 \text{ GHz} = 0.006 \pm 0.0002 \text{ cm}^{-1}$$

$$D_1 = 1.29 \pm 0.015 \text{ GHz} = 0.043 \pm 0.0005 \text{ cm}^{-1}$$

The depth (and area) of burned holes should be related to the burning efficiency of the contributing groups of molecules. A close inspection of Figure 7 and Table 1 shows that the holes assigned to molecules of group 1c are deeper and have larger areas than those assigned to groups 1a and 1b, and holes of these two last groups seemed to have similar areas.

To provide an explanation, we propose a simple kinetic model. We assume that the number of burned molecules from groups 1a, 1b, or 1c is proportional to

$$A_{zi'}k^{\text{isc}}{}_{i'}$$

where i' is the spin sublevels z', x', or y', $A_{zi'}$ is the rate constant for the $T_{0z} \rightarrow T_{1i'}$ absorption, and $k^{\text{isc}}{}_{i'}$ is the intersystem crossing rate constants for the $T_{1i'} \rightarrow S_n$ depopulation. We further assume that the hole-reading process is described by the expression

$$A_{zi'}k^{\text{r}}/k^{\text{isc}}{}_{i'}$$

where k^{r} is the radiative rate constant, equal for all spin sublevels of T_1. We also neglected radiative and internal conversion contributions to the total depopulation rate constant of each spin sublevel of T_1. In other words we replace this rate constant by the dominating intersystem crossing rate. The real hole burning experiment has a contribution from both burning and reading processes, and thus, the areas of satellite holes can be approximated by the following equations:

$$A_{zz'}k^{\text{isc}}{}_{z'}A_{zy'}k^{\text{r}}/k^{\text{isc}}{}_{y'} \propto S_1 = 0.041 \quad (1)$$

$$A_{zz'}k^{\text{isc}}{}_{z'}A_{zx'}k^{\text{r}}/k^{\text{isc}}{}_{x'} \propto S_2 = 0.032 \quad (2)$$

$$A_{zx'}k^{\text{isc}}{}_{x'}A_{zy'}k^{\text{r}}/k^{\text{isc}}{}_{y'} \propto S_3 = 0.031 \quad (3)$$

$$(A_{zz'})^2k^{\text{r}} + (A_{zx'})^2k^{\text{r}} + (A_{zy'})^2k^{\text{r}} \propto S_4 = 0.069 \quad (4)$$

$$A_{zy'}k^{\text{isc}}{}_{y'}\,A_{zx'}k^{\text{r}}/k^{\text{isc}}{}_{x'} \propto S_5 = 0.043 \quad (5)$$

$$A_{zx'}k^{\text{isc}}{}_{x'}A_{zz'}k^{\text{r}}/k^{\text{isc}}{}_{z'} \propto S_6 = 0.033 \quad (6)$$

$$A_{zy'}k^{\text{isc}}{}_{y'}A_{zz'}k^{\text{r}}/k^{\text{isc}}{}_{z'} \propto S_7 = 0.068 \quad (7)$$

From (eq 1)/(eq 2) and (eq 6)/(eq 7), we can obtain $A_{zy'} \approx 1.42A_{zx'}$ and $k^{\text{isc}}{}_{y'} \approx 1.27k^{\text{isc}}{}_{x'}$. From (eq 1)/(eq 3) and (eq 2)/(eq 6), we can obtain $A_{zz'} \approx 1.35A_{zx'}$ and $k^{\text{isc}}{}_{z'} \approx 0.98k^{\text{isc}}{}_{x'}$.

If one accepts the above rates, the predicted area of the central hole (with respect to the area of other holes) should be much larger than that observed. There are two possible explanations for the discrepancy. The experimental spectrum of holes presented in Figure 7 may have been obtained at the fluence saturation condition. To solve this problem, we would have to study the shape of the holes as a function of burning fluence and extrapolate the results to zero fluence. Unfortunately, because of the poor signal-to-noise ratio at low fluence, this extrapolation would be very difficult, and therefore, this experiment was not performed. Alternatively, the fitting procedure may possibly have overestimated the area of the side holes compared with the central hole.

The same pattern of holes as those presented on the right side of Figure 9 can be obtained for a negative value of D_1, when the ordering of spin sublevels energy is $E(T_{1y'}) < E(T_{1x'}) < E(T_{1z'})$. In this case, the same set of equations as eqs 1−7 leads to $A_{zy'} \approx 1.62A_{zx'}$, $A_{zz'} \approx 1.55A_{zx'}$, $k^{\text{isc}}{}_{y'} \approx 0.79k^{\text{isc}}{}_{x'}$, and $k^{\text{isc}}{}_{z'} \approx 1.02k^{\text{isc}}{}_{x'}$. Considering the spectrum of holes alone, it is impossible to decide which energy ordering is correct. The argument to apply one or another order of spin sublevels can be obtained from fluorescence decays. In the case of the pseudo-E/trans conformer of 22-DNC we found that fluorescence decays are composed of one short (5.9 ns) and two long (28.1 ns) time components. The complex decay was interpreted to be a sum

of three independent decays from three different spin sublevels. Thus, one spin sublevel is characterized by fast rate constants of intersystem crossing $k^{isc} = 1/(5.9\ ns) \approx 1.7 \times 10^7\ s^{-1}$, whereas the two other spin levels have much slower $k^{isc} = 1/(28.1\ ns) \approx 3.6 \times 10^7\ s^{-1}$ rate constants (using the assumption that intersystem crossing is the main and dominating channel of the T_1 state depopulation). The situation that one intersystem crossing rate ($k^{isc}_{y'}$) is bigger than two others (which are nearly equal) is predicted by a model where the lowest energy sublevel is the $T_{1z'}$ sublevel and thus a positive D_1 (the competitive model where $T_{1z'}$ is the highest energy spin sublevel predicts that $k^{isc}_{y'}$ is smaller than the other two). As a reminder, the fluorescence decay was best fitted by a three-exponential dependence where the biggest preexponential factor was connected with the shortest decay component (taking into account the Boltzman population of the spin sublevels of T_0 at 5 K). This observation agrees with the prediction of the "hole-burning" model, which gives the highest value for $A_{zy'}$, for the absorption from the lowest energy (and thus the highest population) spin sublevel T_{0z} to the fastest decaying spin sublevel $T_{1y'}$. The agreement, however, is only qualitative because from the analysis of the hole-burning spectrum we obtained $k^{isc}_{y'} \approx 1.27k^{isc}_{x'}$, whereas from fluorescence decays $k^{isc}_{y'} \approx 4.6 \times k^{isc}_{x'}$.

An implication of the simple kinetic model presented above is the possibility of obtaining information about the spatial orientation of the principal spin axes in the T_1 state with respect to the z direction, defined in the ground state. The absorption transition moments are spin-independent, and thus, the partition of the absorption rate constant A into the components $A_{zz'} = 0.34A$, $A_{zx'} = 0.25A$, and $A_{zy'} = 0.41A$ (describing absorption from the T_{0z} to the $T_{1z'}$, $T_{1x'}$, and $T_{1y'}$) should depend on the projection of direction z onto the directions of the new principal spin axes z', x', and y', respectively.

According to the model, each of the deep holes at -13.65 and -14.95 GHz (as well as antiholes on the high-energy side) should be surrounded by narrow satellite holes in a fashion similar to that of the central hole. However, this is not the experimental observation. To explain this result, we have to consider that the frequency position of these holes is mainly determined by the D_0 parameter, which can differ slightly for molecules contributing to the hole. It results in a smoothing of the substructures in the profile of holes.

Finally, let us mention that we observed a magnetic field effect on the shape of the hole-burning spectrum. The result was a smoothing of the holes under increasing magnetic flux up to 320 G, which is a consequence of a lack of macroscopic orientation of carbenes in a Shpolskii matrix. The analysis of the magnetic field effect will be the subject of forthcoming investigations.

V. Conclusion

This work presents and discusses the successful observation of hole burning on the inhomogeneous 0,0 line of the fluorescence excitation spectrum of 22-DNC in *n*-hexane at 1.7 K. The pattern of observed holes was explained assuming that the main depopulation channel of the excited T_1 state was intersystem crossing. Both intersystem crossing steps, $T_1 \rightarrow S_n$ and $S_1 \rightarrow T_0$, contribute to the shape of the hole-burning spectrum. The latter step selectively populates the T_{0z} sublevel, and the only group of molecules that can be burned absorb laser radiation in this state. Another implication of the $S_1 \rightarrow T_{0z}$ polarization is the possibility of the observation of (temporal) antiholes. This unusual observation is probably related to an extremely long spin-relaxation time in the T_0 state. The former intersystem-crossing step contributes to the relative areas of satellite holes surrounding the central hole. Another factor contributing to the areas of these holes originates from the fact that absorption from T_{0z} to different spin sublevels of T_1 is dependent on the projection of direction z onto new directions of the principal spin axes z', x', and y'. Analysis of frequency positions of satellite holes provided the ZFS parameters of the T_0 and T_1 states: $E_0 = 0.022 \pm 0.001\ cm^{-1}$, $D_0 = 0.477 \pm 0.001\ cm^{-1}$, $E_1 = 0.006 \pm 0.0002\ cm^{-1}$, and $D_1 = 0.043 \pm 0.0005\ cm^{-1}$.

22-DNC is the second system where hole-burning spectra have been observed and successfully analyzed, but in this case, in a more elaborate fashion than the previous study of 2-NPC. We think that the hole-burning method has demonstrated useful possibilities in the case of triplet−triplet transitions and should be extended to other systems with the triplet ground states.

References and Notes

(1) (a) Kirmse, W. *Carbene Chemistry*; Academic Press: New York, 1964. (b) *Carbenes*; Jones, M., Jr., Moss, R. A., Eds; Wiley: New York, 1973 and 1975; Vols. I and II. (c) Wentrup, C. *Reactive Molecules*; Wiley: New York, 1984.

(2) Trozzolo, A. M.; Wasserman, E. In *Carbenes*; Moss, R. A., Jones, M., Jr., Eds.; Wiley: New York, 1975; Vol. II, p 185.

(3) Closs, G. L. In *Carbenes*; Moss, R. A., Jones, M., Jr., Eds.; Wiley: New York, 1975; Vol. II, p 159.

(4) Migirdicyan, E.; Kozankiewicz, B.; Platz, M. S. In *Advances in Carbene Chemistry*; Brinker, U., Ed.; JAI Press Inc.: Stamford, CT, 1998; Vol. 2, p 97.

(5) Kozankiewicz, B.; Bernard, J.; Migirdicyan, E.; Orrit, M.; Platz, M. S. *Chem. Phys. Lett.* **1995**, *245*, 549.

(6) Kozankiewicz, B.; Bernard, J.; Migirdicyan, E.; Orrit, M.; Platz, M. S. *Mol. Cryst. Liq. Cryst.* **1996**, *283*, 191; **1996**, *291*, 143.

(7) Prakash, G. K. S.; York, C.; Liao, Q.; Kotian, K.; Olah, G. A. *Heterocycles* **1995**, *40*, 79.

(8) Beckmann, E.; Liesche, O.; Correns, E. *Chem. Ber*. **1923**, *56*, 351.

(9) Jonczyk, A.; Wlostowksa, J. *Synth. Commun.* **1978**, *8*, 569.

(10) Despres, A.; Lejeune, V.; Migirdicyan, E.; Admasu, A.; Platz, M. S.; Berthier, G.; Pariser, O.; Flament, J. P.; Baraldi, I.; Momicchioli, F. *J. Phys. Chem.* **1993**, *97*, 13358.

(11) Kozankiewicz, B.; Despres, A.; Lejeune, V.; Migirdicyan, E.; Olson, D.; Michalak, J.; Platz, M. S. *J. Phys. Chem.* **1994**, *98*, 10419.

(12) Despres, A.; Lejeune, V.; Migirdicyan, E.; Platz, M. S. *J. Phys. Chem.* **1992**, *96*, 2486.

(13) Brandon, R. W.; Closs, G. L.; Hutchison, C. A., Jr. *J. Chem. Phys.* **1962**, *37*, 1878.

(14) Doetschman, D. C.; Botter, B. J.; Schmidt, J.; van der Waals, J. H. *Chem. Phys. Lett.* **1976**, *38*, 18.

(15) McGlynn, S. P.; Azumi, T.; Kinoshita, M. *Molecular Spectroscopy of the Triplet State*; Prentice-Hall: Englewood Cliffs, NJ, 1969.